Environmental effect of steam on crack closure mechanisms of a 9 - 12 % Cr ferritic/martensitic steel

T. Fischer, B. Kuhn

Forschungszentrum Juelich GmbH, Institute for Energy and Climate Research (IEK), Microstructure and Properties of Materials (IEK-2), Juelich, Germany

Abstract

In the present study the impact of steam atmosphere on the threshold value and the active crack closure mechanisms of the ferritic/martensitic steel X20CrMoV12-1 were investigated from 300 °C - 600 °C. This temperature range is of particular importance for flexible power plant operation. The flexibilized operating mode is necessary because of the increased share of renewable sources of energy included in the power grid. Modern thermal power plants must be capable to compensate fluctuations in residual load. This results in a fundamental change in loading and damage scenarios. The start-up and shut-down cycles as well as load fluctuations increased drastically compared to the past. As a consequence the hold time at constant high temperature decreases and the damage scenario changes from creep to fatigue dominated damage or depending on the operating conditions to creep fatigue interaction. Currently original design codes are of limited validity for the assessment of such loading scenarios. For this reason new design codes based on damage tolerance concepts are required to exploit the maximum component lifetime without reducing safety. It was demonstrated that the steam atmosphere leads to an increase in the threshold value in the relevant temperature range and thus offers additional lifetime potential. This increase in threshold with rising temperature was correlated with increasing oxide layer thickness. Furthermore the active crack closure mechanisms were separated and quantified up to 400 °C (limited by the determination of the intrinsic threshold value). In addition the impact of temperature and corrosion on the threshold value was separated and quantified despite superposition of several mechanisms.

Keywords: Threshold, Steam atmosphere, Temperature, Crack closure mechanism, 9 - 12 % Cr steels

1. Introduction

At present, the operation of fossil fuel power plants has changed from base load to flexible residual load. This means that modern power plants must be able to close the supply gap that cannot be provided by renewable sources of power. The associated mandatory increase in the number of start-up and shut-down cycles and the resulting temperature and internal pressure fluctuations cause increased wear of structural materials. Fatigue damage due to increasing alternating load thus is of enormous importance for power plant operators, whereas the influence of creep is reduced because of shorter dwell times at constant high operating temperatures. Current design codes are of limited validity for the assessment of

such loading scenarios. Fracture mechanical crack growth analysis provides an effective way of assessing high degrees of fatigue of components subject to cyclic loading. In addition to code-based fatigue analysis this allows for additional utilization of component service life without reducing the required safety margins. THERRI (German: THermisches ERmüdungsRIsswachstum, engl.: Thermal fatigue crack propagation), a national, joint research project (funded under grant number 03ET7024A by the German Federal Ministry of Economic Affairs and Energy) under leadership of TÜV NORD GmbH was initiated in 2013. The main goal was to develop a draft directive [1] for the application by technical surveillance authorities. For this purpose the focus of research was on fatique/creep-fatique crack growth behavior in X20CrMoV12-1 (a tempered 12% Cr ferritic-martensitic steel widespread in the German power industry [2, 3]). Experiments were carried out covering cycling frequency [4], the implementation of dwell times [4], the influence of atmosphere (steam) [5], an analysis of the application limit [6] of the K-concept [7] and the threshold behavior, including the investigation of the corresponding crack closure mechanisms in the temperature range from 300 °C - 600 °C in air [8]. P. Porkorný et. al. [9] for railway axle steel EA4T found oxide induced crack closure to be the most significant crack closure mechanism, causing an enormous increase in residual fatigue life time, in air (relative humidity of 30 - 40 %) at ambient temperature and. For a relative humidity of 4 -11% a 2.7 MPa√m lower threshold value was measured compared to air. For an initial crack length of 1 mm this results in a more than 200 times shorter residual fatigue lifetime. This underlines the strong influence of atmosphere on residual fatigue lifetime. In order to exploit the lifetime potential of power plant components to the maximum without reduction in safety, it is necessary to deeply investigate the temperature dependent threshold behavior and to understand the crack closure mechanisms of structural materials in steam. For this reason, it was examined to what extent the experimental approach to separation and quantification of the crack closure mechanisms, published in [8], is transferable to experiments carried out in steam. In general thick-wall components (e.g. spheroidal forgings, fittings, collectors, pumps, turbine bypass valves (TBV)) are from particular importance, as they are exposed to particularly high cyclical loads. The investigation was conducted in accordance with our previous studies [8] on X20CrMoV12-1 extracted from an ex-service TBV (operation duration ~21 years), the plant component facing the most damaging loading scenario in flexible operation.

In the near-threshold region the crack growth behavior in gaseous atmospheres is controlled by two opposing mechanisms: On the one hand the corrosion fatigue processes (e.g. hydrogen embrittlement), which accelerate crack growth. On the other hand the resulting crack closing mechanisms, which decelerate crack propagation [10]. **Figure 1** schematically shows the mechanism of accelerate crack propagation caused by embrittlement of Fe by H.

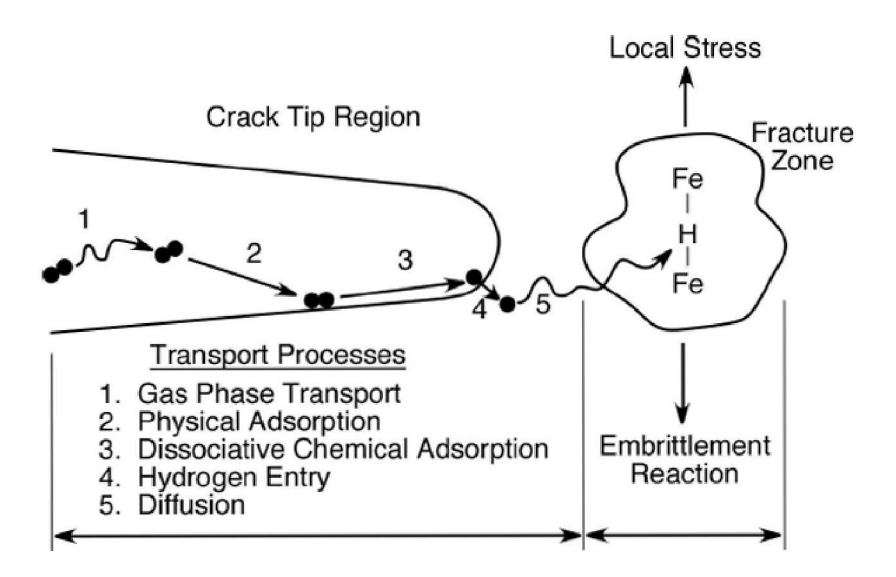


Figure 1: Schematic illustration of the different process steps necessary for accelerated crack propagation in case of H-embrittlement of Fe [11].

Because the crack tip is exposed to an atmosphere there are at least seven different types of processes, that can occur and each can be determining for the rate of crack growth: The first process is bulk mass transport of the atmosphere to the crack tip (1). Subsequently, surface adsorption occurs at, and in the vicinity, of the crack tip (2). Then there is surface diffusion to the crack tip (3). In the next process step surface chemical reaction(s) take place (4), followed by volume diffusion ahead of the crack tip (5). This leads to embrittling reaction(s) in the material bulk (6) and subsequently to fracture (7). The rate of adsorption of atoms of atmosphere species at the crack tip also may be a rate determining step. For example, in a gaseous atmosphere this can be the rate of atoms impinging on the crack tip surfaces [11].

Crack closure is an important mechanism responsible for deceleration of crack propagation. The crack closing mechanisms known today include oxide induced crack closure [12-14], plasticity induced crack closure [15, 16], crack surface roughness [17], viscous-fluid induced and material phase transformation induced crack closure [18]. Obviously oxide-induced crack closure is the most import mechanisms in steam. Oxides and other corrosion products can cause oxide-induced crack closure. These products can lead to an increase in volume in the vicinity of the crack tip and at the crack faces, which can result in premature contact of the crack face with (partial) unloading from tension and thus lead into a reduction of the effective stress intensity range [19]. Temperature and oxygen partial pressure of the surrounding atmosphere have an important impact on oxide induced crack closure. If temperature and oxygen partial pressure increase the extent of oxide induced crack closure rises due to accelerated oxidation of the crack faces [20-22]. The impact of gaseous and aqueous atmospheres on crack propagation behavior of high strength steels s is schematically shown in Figure 2 [23]. Under the condition $K_{max} > K1_{SCC}$ (subscript denotes stress corrosion cracking in mode I) an aggressive atmosphere leads to a crack propagation rate accelerated by several orders of magnitude. The acceleration of fatigue fracture is more pronounced at lower frequencies because atmosphere has more time to interact with the crack tip per load cycle. The threshold value at which stress corrosion fatigue begins to affect the crack growth rate decreases with increasing R-ratio, because $K_{max} (= \frac{\Delta K}{1-R})$ approaches K_{ISCC} at lower K values under these conditions.

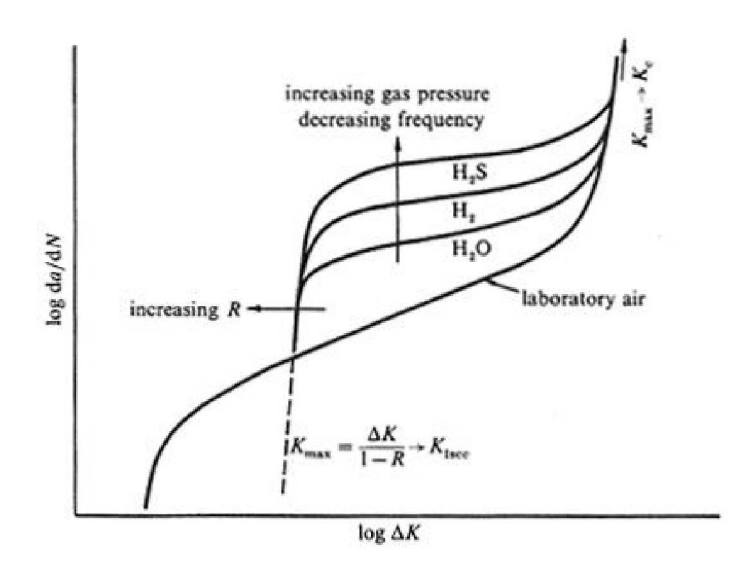


Figure 2: Schematic representation of the impact of atmosphere, testing frequency and R-ratio on crack propagation behavior of high-strength steel [23].

In low carbon steel Konami [24] observed a decelerating effect of salt water on crack growth rate in comparison to air. The reason for this phenomenon were corrosion products, filling the crack, which led to a reduction in ΔK_{eff} (subscript denotes effective). **Figure 3** depicts the threshold behavior of Cr - Mo - V (A 470-74) rotor steel under load control at R = 0.1 in air and steam [25]. Again, in the more corrosive steam medium, a 1.1 MPa \sqrt{m} higher threshold value (ΔK_{th}) was measured than in air. **Figure 4** displays the temperature influence on the threshold behavior of a pressure vessel steel [20]. At R = 0.1, the threshold decreases from 24 °C to 200 °C as the temperature increases, while in contrast a further increase from

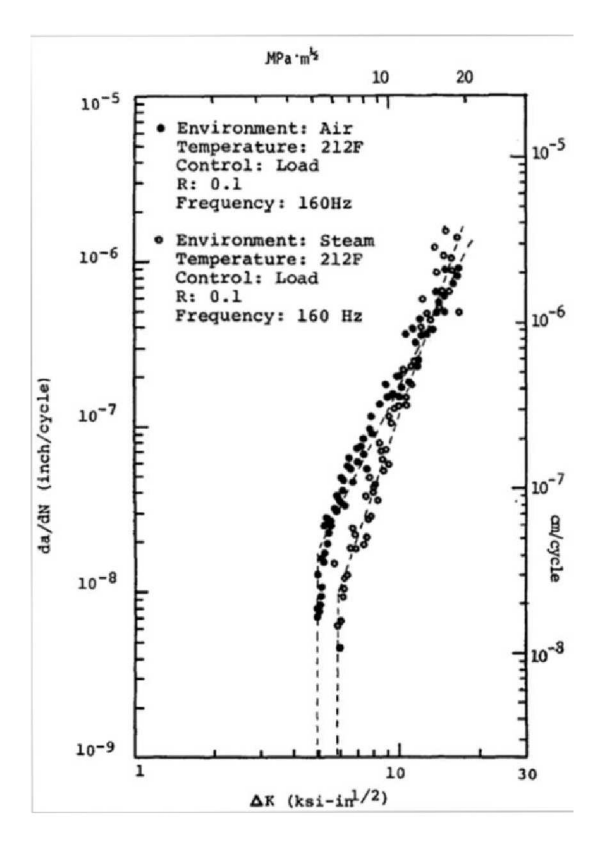


Figure 3: Threshold behavior of Cr - Mo - V (A 470-74) rotor steel in air and steam at 100 °C [25].

200 °C to 343 °C increases the threshold again, while the threshold value at R = 0.7 was independent of temperature. Obviously the impact of temperature decreases with increasing R-ratio. This behavior was attributed to the crack closing mechanisms. This underlines the relevance of the present study, which was performed from 300 °C - 600 °C at R = 0.1 in steam, in terms of utilization of the maximum component life time.

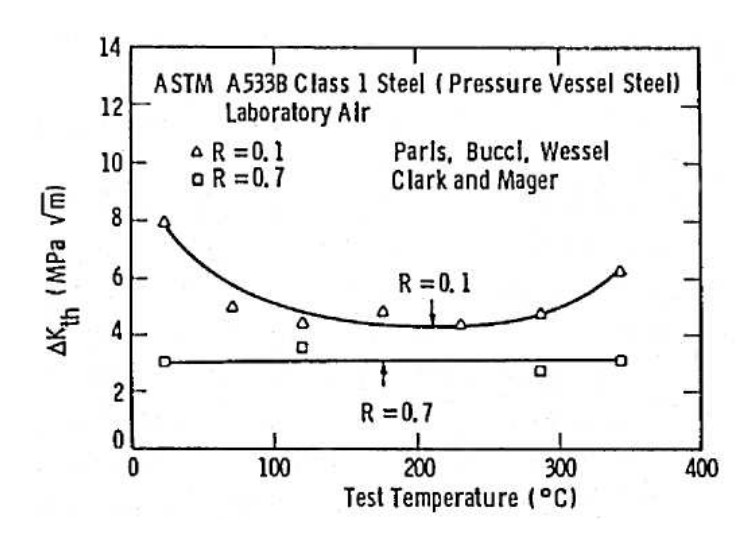


Figure 4: Impact of temperature on ΔK_{th} [20] of ASTM A533B class 1 steel.

In steam an increasing proportion of oxide-induced crack closure is expected with rising temperature, because the 9 - 12 % Cr steels in general oxidize faster in steam than in air [26, 27]. Moreover X20 steel in Ar+50 vol.% H₂O has an anomalous temperature dependence [28] of oxide growth in the temperature range from 550 °C to 650 °C, i.e. the oxidation rate does not rise steadily with increasing temperature. The anomalous/bell-shaped temperature dependence results from the faster diffusion of Cr in the alloy towards the oxidation front with increasing temperature [29-31]. Furthermore the oxide scale growth is probably faster under extrinsic tensile stress. As a consequence of the extrinsic tensile stress the hydrostatic pressure in the oxide may decrease, or under thermodynamic aspects, the free volume in the lattice may rise (described in detail for binary oxides by Pieraggi [32]). The intrinsic stress state strongly influences the chromium transport into and through the oxide scale [33, 34]. Thereby intrinsic chromium vacancy concentration and mobility of chromium vacancies are increased in the chromia scale due to extrinsic stress. Hence, it can be assumed that the complex oxidation behavior of X20 steel in steam has a significant influence on oxideinduced crack closure (particularly at low crack propagation rate) and for this reason could be beneficial especially in the near threshold region. The underlying transport mechanisms in the oxide scales, as well as the effect of superimposed mechanical stress, are not yet nearly understood. The aim of the presented work was to provide basic understanding of the mechanisms occurring in the near-threshold range in steam and to exploit potential, additional lifetime reserves without reduction in safety. In order to develop new models to describe the impact of the different superposing crack closure mechanisms as well as the influence of corrosion and mechanical issues on the threshold behavior in dependence of atmosphere, a validated experimental methodology is necessary. An experimental procedure, which covers the outlined interactions and increases the amount of available data is provided in the present study.

2. Material and Methods

The crack propagation behavior was investigated like in our previous studies [4, 5] on material taken from an ex-service turbine bypass valve (TBV). **Table 1** shows the chemical composition.

Table 1: Chemical composition of X20CrMo V12-1 to standard DIN 17175 (in wt %):

	С	Si	Mn	Р	S	Cr	Мо	Ni	V
X20CrMo V12-1	0.17	≤0.50	≤1.00	≤0.030	≤0.030	10.00	0.80	0.30	0.25
	0.23					12.50	1.20	0.80	0.35

The compact tension (CT) specimen geometry had to be modified due to TBV flange dimensions. Therefore a width of W = 40 mm and thickness of B = 10 mm and an initial notch depth of $a_0 = 10$ mm in accordance with the ASTM test standard [35] was chosen. For the reasons of comparability, the experimental material was taken from the "cold flange" region. This material was in a "virgin" state, because it was not exposed to steam and no mechanical or microstructural degradation could be detected by tensile testing at temperatures up to 600 °C and observation of the martensitic lath structure [4].

Details on the experimental setup and testing technology for crack propagation testing in air [4] are oultined in [5]. All threshold experiments in air and steam (Ar+50 vol.% H_2O) were performed at 20 Hz and R = 0.1. The only exception in terms of load ratio were the intrinsic threshold experiments (testing method described in [8]). The threshold value measurements were conducted by stepped force shedding according to ASTM E647-11 [35], the intrinsic threshold values were acquired applying the ASTM E647-11 approved $K_{l,max}$ method [35]. The measurement of oxide layer thickness is described in [5].

For microstructure investigation a Zeiss Merlin field emission scanning electron microscope (FESEM) was used. EDX (energy dispersive X-ray) detectors from Oxford Instruments, model X-Max 50 and X-Max 80 were applied for the analysis of the chemical composition of the oxide layers.

3. Results and Discussion

3.1 Impact of steam on the threshold value (300 $^{\circ}\text{C}$ - 600 $^{\circ}\text{C}$) and experimental limitations

Despite variations in testing load no consistent crack growth could be measured at 600 $^{\circ}$ C. For this reason, the experiment was terminated and the surface of the CT specimen was examined using scanning electron microscopy (SEM). On the specimen surface, pronounced needle-shaped oxide formation was observed along the flanks and at the tip of the crack (**Figure 5**).

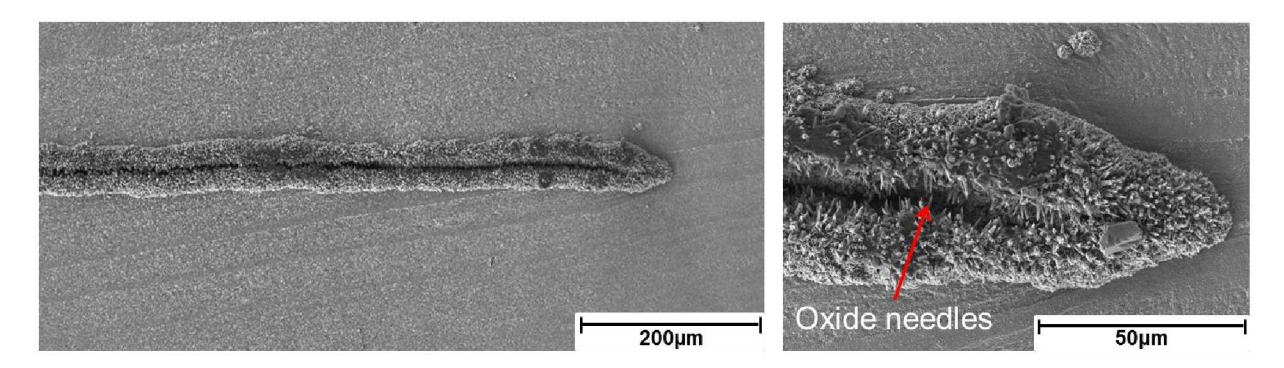


Figure 5: Longitudinal views of the crack tip of the CT specimen from the threshold experiment at 600 °C in steam.

For further analysis, the CT specimen was ground to half the specimen width (5 mm) and SEM examination was performed. **Figure 6** exhibits the crack tip being completely oxidized even in the middle (half thickness) of the specimen. EDX examination confirmed the inner layer to consist of Fe_3O_4 , the outer layer of Fe/Cr-mixed

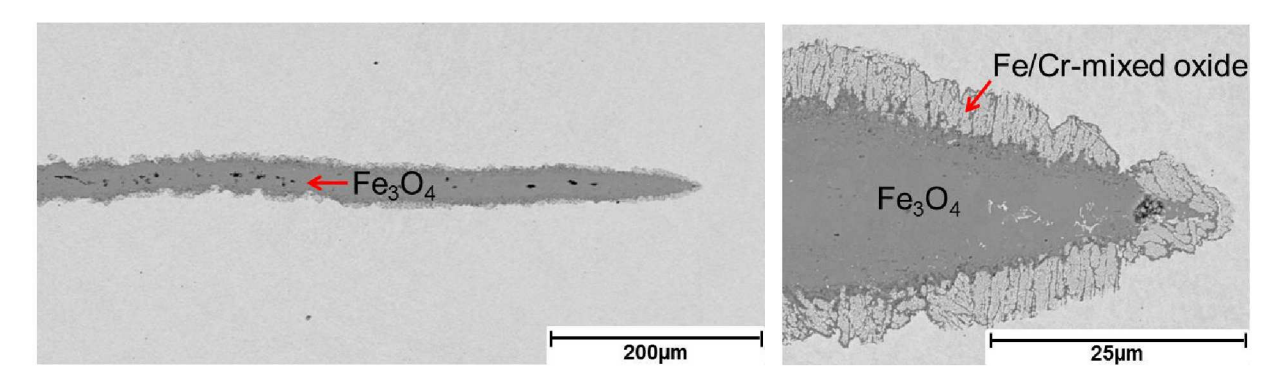


Figure 6: Longitudinal view of the crack tip in the bisected CT specimen from the threshold experiment at 600 $^{\circ}$ C in steam.

oxides. Due to pronounced oxidation at 600 °C determination of the threshold value was impossible. Therefore threshold value experiments were exclusively carried out up to 550 °C. To investigate the impact of steam atmosphere on threshold behavior, experiments were carried out in air for comparison purposes (**Figure 7** and **Table 2**). In the temperature range from 400 °C to 550 °C the threshold values were approximately in the order of 7.9 MPa \sqrt{m} (**Table 2**).

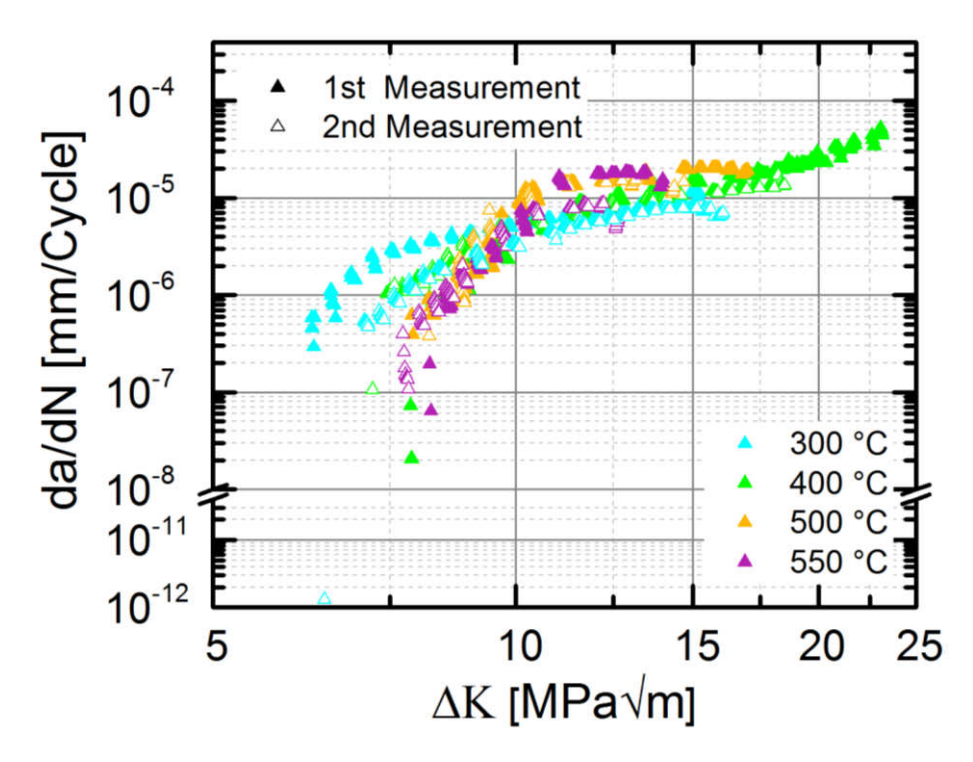


Figure 7: Threshold value experiments in air (f = 20 Hz, T: 300 - 550 ℃; 1st measurements replotted from [8]).

A significant increase of the threshold value was encountered with a rise in temperature from 300 $^{\circ}$ C to 400 $^{\circ}$ C (cf. **Table 2**). The main reason for this was oxide induced crack closure [8].

Table 2: Threshold values determined in air (f = 20 Hz, T: 300 $^{\circ}$ C - 550 $^{\circ}$ C).

Temperature [°C]	300	400	500	550
$\Delta K_{th.}^{1st*}[MPa\sqrt{m}]$	6.3	7.9	7.9	8.2
$\Delta {K_{th.}}^{2nd} \; [MPa\sqrt{m}]$	6.5	7.2	8.2	7.8
*[8]				

Figure 8 compares the threshold value experiments carried out in air and steam. In steam the cyclic crack growth curves drop more abruptly at temperatures lower than 400 ℃ than in air (**Figure 8**). The corresponding threshold values are summarized in **Table 3**. Despite the aggressive steam atmosphere good reproducibility of the experiments was achieved (cf. **Figure 8** and **Table 3**).

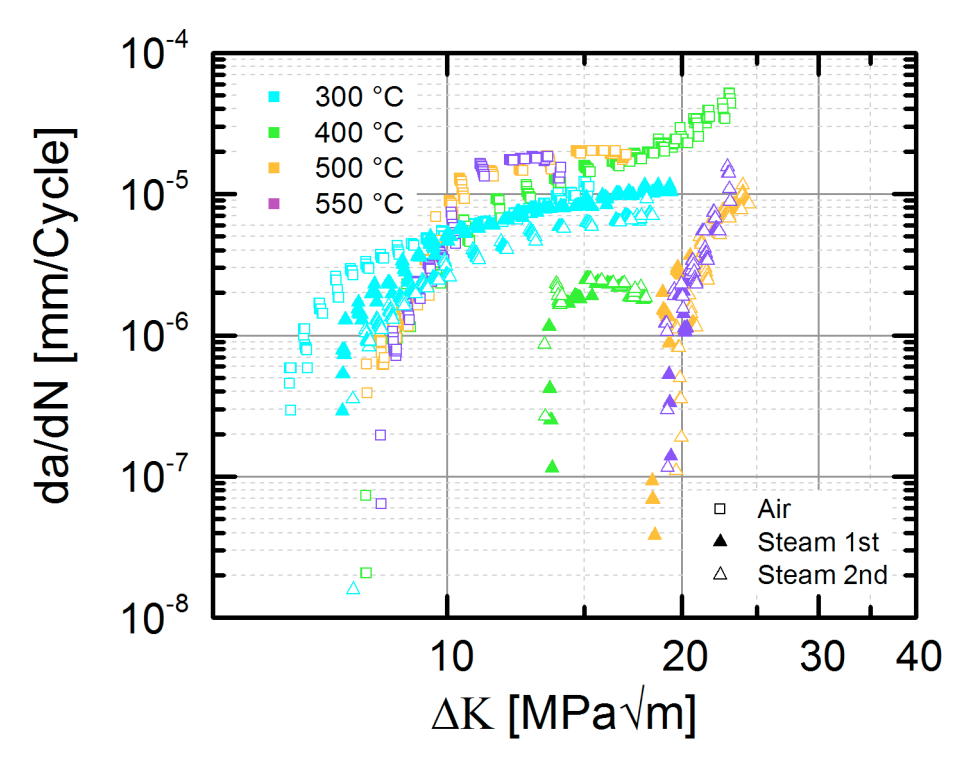


Figure 8: Comparison of the threshold value experiments executed in air and steam (f = 20 Hz, T: 300 - 550 °C).

The impact of steam atmosphere on the threshold value was perceivable at 300 $^{\circ}$ C already. The threshold value in steam at 300 /400 / 500 / 550 $^{\circ}$ C increased (comparison of averaged thresholds) by $\sim 1.1/\sim 6/\sim 11/\sim 11.3$ MPa \sqrt{m} (**Figure 9**). Upon a temperature increase from 300 $^{\circ}$ C to 500 $^{\circ}$ C, the threshold value in steam raised on average by ~ 11.9 MPa \sqrt{m} .

Table 3: Threshold values in steam (f = 20Hz, T: 300 $^{\circ}$ C - 550 $^{\circ}$ C).

Temperature [°C]	300	400	500	550
ΔK _{th.} 1st [MPa√m]	7.3	13.6	18.5	19.4
$\Delta K_{th.}{}^{2nd} \; [MPa\sqrt{m}]$	7.6	13.4	19.7	19.2

3.2 Correlation of threshold values and oxide scale thickness.

The higher threshold values in steam can be correlated with increasing oxide scale thicknesses (**Figure 10**). Upon a temperature increase from 300 °C to 400 °C the average oxide scale thickness increased by approx. 2.14 μ m, while the average threshold value increased by ~ 6 MPa \sqrt{m} . Upon further temperature increased from 400 °C to 500 °C, the average

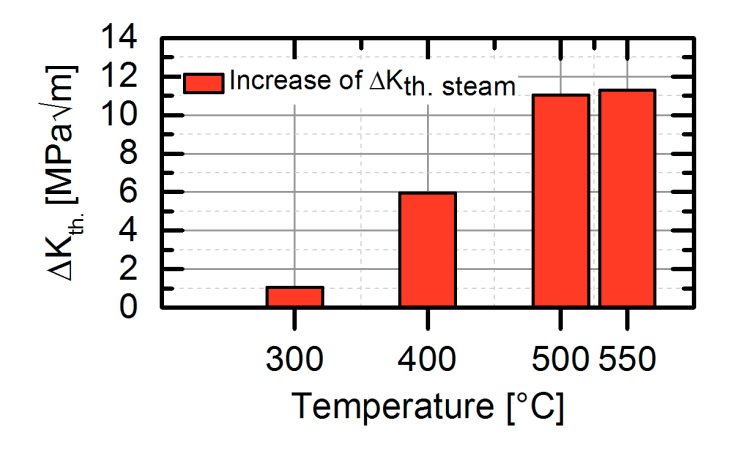


Figure 9: Threshold value increase in steam compared to air (300 $^{\circ}$ C - 550 $^{\circ}$ C).

oxide scale thickness grew by approximately 5.54 μ m, while the threshold value gained by an average of 5.6 MPa \sqrt{m} . From 300 - 500 °C a good correlation between oxide scale growth and increasing threshold was found, but further increase in temperature to 550 °C caused a comparatively small gain in threshold of 0.2 MPa \sqrt{m} , while the average oxide scale thickness increased by approx. 3.4 μ m. At temperatures exceeding 500 °C increased oxidation obviously does not play a significant role in threshold behavior anymore. This saturation was caused by the crack being completely filled with oxides. In this case further increase in oxide scale thickness (with temperature) does not lead to further premature contact of the crack edges anymore.

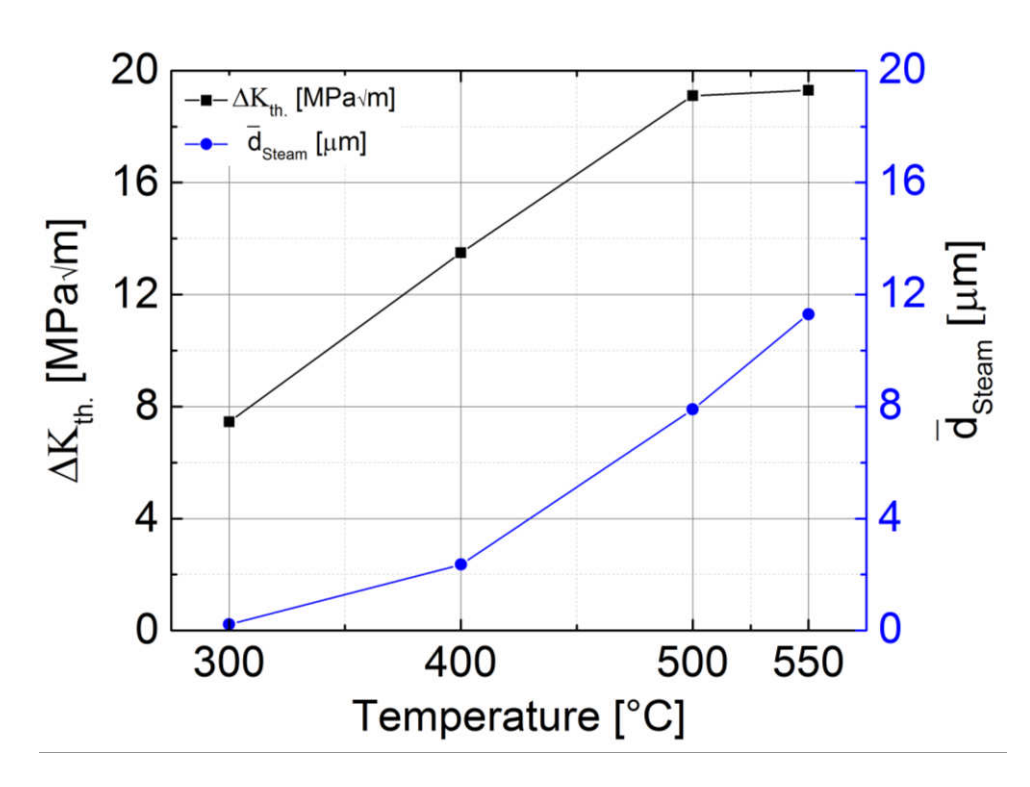


Figure 10: Threshold value and average oxide scale thickness in dependence of temperature (\overline{d}_{Steam} = average oxide scale thickness).

3.3 Distinction and quantification of crack closure mechanisms in steam and application limitations

To separate and quantify the responsible mechanisms (crack closure, corrosion and pure temperature influence) governing the threshold behavior in steam, the experimental method developed in air or rather the evaluation from our previous study [8] was slightly modified. The conditions for the applicability of the methodology were described in [8]. In **Table 4** the required threshold (ΔK_{th}) and intrinsic thresholds values (ΔK_{th} intrinsic) in air, vacuum and steam (subscripted as air, vacuum and steam) are listed. In contrast to the threshold value, the intrinsic threshold value was determined at constant K_{max} , while amplitude ΔK was reduced by linearly increasing K_{min}, until crack growth no longer occurred (K_{max}-method [35]). Using this method, the threshold value was determined at high R-ratios (close to 1) so that the crack is fully opened. For this reason any crack closing effects can be excluded [36]. It was outlined in our previous study [8] why the comparison of threshold values determined at different R ratios is permissible. The intrinsic threshold value in steam could only be determined up to 400 °C, because the oxide scale was too thick to determine an intrinsic value. Consequently, the methodology can only be applied up to 400 °C in steam (in this case), or more generally speaking, as long as the determination of intrinsic threshold values is possible. Oxide- and plastically induced crack closure occur in the threshold value experiments in air and steam (**Table 5**). The size ratio $S_R = d / r_p$ (with d specifying the characteristic microstructural distance and rp the size of the plastic zone) [37] was used to estimate the relevance of roughness induced crack closure. With S_R ≥ 1 the influence of roughness induced crack closure is decisive, for $S_R \ll 1$ it is negligible. The physical background for these assumptions are described in [37]. In our previous study [8] on the same material it was determined that $S_R \ll 1$. For this reason roughness-induced crack closure was considered to be of minor relevance. Furthermore, it was assumed that oxide induced crack closure dominated above roughness induced crack closure, because of the high oxide scale thickness (cf. Figure 10) encountered in steam. Additionally, the corrosive

Table 4: Threshold and intrinsic threshold values in air, vacuum and steam from 300 ℃ - 400 ℃.

	ΔK _{th. Air} * [MPa√m]	ΔK _{th. Air} (intrinsic) [MPa√m]	ΔK _{th. Steam} [MPa√m]	ΔK _{th. Steam} (intrinsic) [MPa√m]	ΔK _{th. Vacuum} * [MPa√m]	$\Delta K_{ ext{th. Vacuum}}$ (intrinsic) $$ [MPa \sqrt{m}]
300 °C	6.3	4.0	7.6	4.4	9.5	7.6
400 °C	7.9	4.2	13.6	4.4	8.4	6.8

^{*[8]}

impact of steam will occur, which leads to the reduction in threshold value (cf. introduction section). In the intrinsic threshold value experiments a corrosive impact of steam was active only (**Table 5**).

Table 5: Relevance of crack closure mechanisms and corrosion impact in different types of threshold experiments carried out in steam.

	Corrosion	Oxid-induced crack	Plastic-induced crack	
		closure	closure	
ΔK _{th. Steam}	-	+	+	
ΔK _{th. Steam (intrinsic)}	-			

 $^{- = \}Delta K_{th} \downarrow$, $+ = \Delta K_{th} \uparrow$

Accordingly, the corrosive impact of steam can be calculated from the difference between the intrinsic threshold values measured in vacuum and steam:

$$\Delta K_{Corrosion \ steam} = \Delta K_{th. \ Vakuum \ intrinsic} - \Delta K_{th. \ Steam \ intrinsic}$$
 (1)

The proportion of plastically-induced crack closure can be determined as follows [8]:

$$\Delta K_{Plastic-induced} = \Delta K_{th. \ Vacuum} - \Delta K_{th. \ Vaccum \ intrinsic}$$
 (2)

The threshold value in steam is composed of the intrinsic threshold value in vacuum, the crack closing mechanisms, minus the impact of corrosion:

$$\Delta K_{th. Steam} = \Delta K_{th. Vacuum intrinsic} + \Delta K_{Oxide-induced} + \Delta K_{Plastic-induced} - \Delta K_{Corrosion steam}$$
(3)

The influences of the individual mechanisms, calculated applying equations 1-3, are listed in **Table 6.** The corrosion impact was about 1.2 MPa \sqrt{m} lower at 400 °C than at 300 °C. The same trend was overserved in air. The influence of corrosion in air was 3.6 MPa \sqrt{m} at 300 °C and 2.6 MPa \sqrt{m} at 400 °C [8]. The relatively short testing time may be considered to be a possible reason for the insensitivity of the corrosion impact to atmosphere in the temperature range from 300 °C to 400 °C. The extent of plastically-induced crack closure was assumed to be insensitive to atmosphere. The proportion was 1.9 / 1.6 MPa \sqrt{m} at 300 / 400 °C [8]. The share of oxide induced crack closure was 1.7 / 7.6 MPa \sqrt{m} at 300 / 400 °C in steam, which was considered to be the main cause of the significant threshold increase from 300 to 400 °C. In steam, the proportion of oxide induced crack closure was significantly higher than in air ($\Delta K_{\text{Oxide-induced 300 °C Air}$: 0.4 MPa \sqrt{m} , $\Delta K_{\text{Oxide-induced 400 °C Air}$: 2.1 MPa \sqrt{m} [8]). Consequently, oxide induced crack closure was responsible for the higher threshold values in steam.

Table 6: Quantitative proportions of crack closure mechanisms, impact of corrosion and effect of temperature from 300 ℃ - 400 ℃.

Mechanisms	ΔK _{corrosion} [MPa√m]	ΔK _{Plastic-induced} [MPa√m]	ΔK _{Oxide-induced} [MPa√m]	Temperature influence [MPa√m]	Summation [MPa√m]
Temperature					
300 ℃	3.6	1.9	1.7	7.6	-
400 °C	2.4	1.6	7.6	6.8	-
Δ ₃₀₀ °C→ 400 °C	1.2	-0.3	5.9	-0.8	6

A comparison of oxide scale thicknesses and crack tip opening displacements (CTOD; cf. **Table 7**) demonstrates the effectiveness of oxide induced crack closure in steam: While the ratio of average oxide scale thickness to CTOD was ~ 1.45 at 300 °C, it rose to ~ 4.23 at 400 °C. In contrast, in air this ratio changed from ~ 1.15 at 300 °C to ~ 1.8 at 400 °C only.

Table 7: Oxide layer thickness and crack tip opening displacement (CTOD) in steam from 300 ℃ - 400 ℃.

Temperatur [℃]	R	Yield stress [MPa]	Y [GPa]	ΔK _{th.} [MPa√m]	Average oxide layer thickness [µm]	CTOD ^{**} [μm]
300	0.1	490 [*]	190 [*]	7.6	0.220	0.152
400	0.1	446 [*]	182 [*]	13.6	2.360	0.558

^{*[4] . **}CTOD = 0.49 $\Delta K^2/2\sigma_{Ys}Y$ [38].

4. Conclusion

In our previous study [8] the threshold behavior depending on frequency of the ferritic/martensitic steel X20CrMoV12-1 (relevant temperature range for flexibly operated power plants) was investigated in detail from 300 °C - 600 °C. Furthermore an experimental approach was developed to separate and quantify the relevant crack closure mechanisms.

In the present study, the focus of research was put on the threshold behavior in steam to exploit the maximum material lifetime potential without a dropback in reliability. Furthermore, it was examined whether the experimental approach of separation and quantification crack closure mechanisms, developed in [8], could be applied to experiments in steam with minor modifications.

The following main conclusions can be drawn from the experimental data and corresponding microstructural observation:

- In steam a comparatively small threshold value increase of ~1.1 MPa√m (compared to air) was measured at 300 °C. At 400 °C, 500 °C and 550 °C the increase became significant (~6/ ~11/ ~11.3 MPa√m). This demonstrates an enormous, hidden lifetime potential. In particular P. Porkorný et. al. [9] found a more than 200 times higher residual fatigue life

time caused by an increase in threshold of just 2.7 MPa√m (for an initial crack length of 1 mm).

- The increased threshold values in steam can be correlated with increasing oxide scale thickness. From 500 ℃ the average oxide layer thickness continued to increase significantly while the threshold value remained merely unchanged. Consequently, the threshold value was saturated from 500 ℃ onwards.
- Up to 400 ℃, the crack closing mechanisms and the influence of corrosion could be separated and quantified. In steam the experimental approach of separation and quantification of crack closure mechanisms is limited to 400 ℃, because the formation of prohibitively thick oxide scales prevented the determination of the intrinsic threshold value at 500 ℃. The methodology proved to be applicable as long as the determination of intrinsic threshold values was possible.
- In steam, pronounced oxide-induced crack closure caused higher threshold values with increasing temperature.
- By comparison of the crack closing mechanisms occurring in air and steam from 300 ℃ to 400 ℃ it was demonstrated that oxide-induced crack closure was considerably more effective in steam. This was additionally verified by comparison of the average oxide scale thickness to the CTOD.

Acknowledgments

The authors gratefully acknowledge the German Federal Ministry for Economic Affairs and Energy for supporting this study under grant No. 03ET7024A. In addition, the authors would like to acknowledge the support of B. Werner, H. Reiners and D. Liebert in mechanical testing, V. Gutzeit and J. Bartsch in sample preparation and Dr. E. Wessel for performing the microstructural investigations.

References

- [1] Schulz A, Czubanowski M, Mathes F, Rieck D. Verbundprojekt THERRI Ermittlung von Kennwerten zur Bewertung thermischen Ermüdungsrisswachstums in Kraftwerken. Teilprojekt 4: Numerische Untersuchungen, zerstörungsfreie Prüfmethoden sowie Regelungen zur Bewertung thermischen Ermüdungsrisswachstums in Kraftwerken. FKZ 03ET7024D. Abschlussbericht. TUV Nord EnSys GmbH & Co. KG, Hamburg (Hrsg.). Hannover: Verl. TUV Nord; 2017.134, 98 S., ISBN 978-3-939002-00-0.
- [2] Eggeler G, Nilsvang N, Ilschner B. Microstructural changes in a 12% chromium steel during creep. Steel Res 1987;58–2:97–103.
- [3] Maruyama K. Strengthening mechanisms of creep resistant tempered martensitic steel. ISIJ Int 2001;41:641–53.
- [4] Fischer T, Kuhn B. Frequency and hold time influence on crack growth behavior of a 9–12% Cr ferritic martensitic steel at temperatures from 300 ℃ to 600 ℃ in air. Int J Fatigue 2018;112:165–72.
- [5] Fischer T, Kuhn B. Influence of steam atmosphere on the crack propagation behaviour of a 9–12% Cr ferritic/martensitic steel at temperatures from 300 °C to 600 °C depending on frequency and hold time. Int J Fatigue 2019;119:62–77.

- [6] Fischer T, Kuhn B. Impact of frequency, hold time and atmosphere on creep-fatigue of a 9–12% Cr steel from 300 ℃ to 600 ℃. Int J Fatigue 2019.
- [7] Irwin GRJ. Appl Mech 1957;24:S.361.
- [8] Fischer T, Kuhn B. New insights into the threshold behavior of a 9–12% Cr ferritic/martensitic steel separation and quantification of crack closure mechanisms. Int J Fatigue 2019;127:479–87.
- [9] Pokorny P, Vojtek T, Nahlik L, Hutař P. Crack closure in near-threshold fatigue crack propagation in railway axle steel EA4T. Eng Fract Mech 2017;185:2–19.
- [10] Suresh S, Ritchie R. Near-threshold fatigue crack propagation: a perspective on the role of crack closure; 1983.
- [11] Ricker R, Duquette D. The role of environment in time dependent crack growth, in; 1982. p. 29–48.
- [12] Suresh S, Zamiski GF, Ritchie RO. Oxide induced crack closure: an explanation for near-threshold corrosion fatigue crack growth behavior. Metall Trans A 1981;12(1981):1435–43.
- [13] Suresh S, Ritchie RO. Some considerations on the modelling of oxide-induced fatigue crack closure using solutions for a rigid wedge inside a linear elastic crack. Scripta Metall 1983;17:575–80.
- [14] Fleck NA. Fatigue crack growth: the complications. In: Smith RA, editor. Proc fatigue crack growth, Pergamon; 1986. p. 75.
- [15] Elber W. Eng Fract Mech 1970;2:37-45.
- [16] Elber W. The significance of fatigue crack closure. Damage Tolerance in aircraft structures, Philadelphia: American Society for Testing and Materials; 1971. p. 239–42, ASTM STP486.
- [17] Suresh S, Ritchie RO. A geometric model for fatigue crack closure induced by fracture surface roughness. Metall Trans A 1982;13A:, p. 1627–31.
- [18] Suresh S. Fatigue of materials. 2nd ed. Cambridge: Cambridge University Press; 1998.
- [19] Pippan R, Hohenwarter A. Fatigue crack closure: a review of the physical phenomena. Fatigue Crack Closure 2017.
- [20] Liaw PK. Overview of crack closure at near-threshold fatigue crack growth levels. In: Mechanics of fatigue crack closure, ASTM International; 1988.
- [21] Petit J, Zeghoul A. On the effect of environment on short crack growth behaviour and threshold. In: Miller KJ, de los Rios ER, editors. Proc the behaviour of short fatigue crack, ESIS, London; 1986. p.163.
- [22] Petit J, Mendenz J, Barata W, Legendre L, Muller C. Influence of environment on propagation of short fatigue cracks in a titanium alloy. In: Miller KJ, de los Rios ER, editors. Proc short fatigue cracks, ESIS 13, Mechnical Engineering Publications, London; 1992. p. 235.
- [23] Suresh S. Fatigue of materials. Fatigue Mater; 2004.
- [24] Konami K. Corrosion fatigue crack retardation and enhancement and fracturesurface reconstruction technique. In: Scott P, Cotis RA, editors. Environment Assisted Fatigue, EGF7, Mechanical Engineering Publications, London; 1990. p. 189–204.
- [25] Tu LKL, Seth BB. Threshold corrosion fatigue crack growth in steels. J Test Eval, JTEVA 1978;6(1):66–74.
- [26] Hansson AN, Montgomery M, Somers MAJ. Oxidation of X20 in water vapour: the effect of temperature and oxygen partial pressure. Oxid Met 2009;71:201.
- [27] Jianian S, Longjiang Z, Tiefan L. High-temperature oxidation of Fe-Cr alloys in wet oxygen. Oxid Met 1997;48:347–56.
- [28] Zurek J, Wessel E, Niewolak L, Schmitz F, Kern TK, Singheiser L, et al. Anomalous temperature dependece of oxidation kinetics during steam oxidation of ferritic steels in the temperature range 550–650 °C. Corros Sci 2004;46:2301–17.
- [29] Nickel H, Wouters Y, Thiele M, Quadakkers WJ. The effect of water vapor on the oxidation behavior of 9%Cr steels in simulated combustion gases. Fresenius' J Anal Chem 1998;361:540–4.

- [30] Żurek J, Wessel E, Niewolak L, Schmitz F, Kern TU, Singheiser L, et al. Anomalous temperature dependence of oxidation kinetics during steam oxidation of ferritic steels in the temperature range 550–650 °C. Corros Sci 2004;46:2301–17.
- [31] Quadakkers WJ, Ennis PJ, Zurek J, Michalik M. Steam oxidation of ferritic steels laboratory test kinetic data. Mater High Temp 2005;22:47–60.
- [32] Pieraggi B. Defects and transport in oxides and oxide scales. In: Richardson JA. Shreir's corrosion, Vol. I, Elsevier, Amsterdam; 2010. p. 102.
- [33] Hansel M, Turan E, Shemet V, Gruner D, Breuer U, Simon D, Gorr B, Christ H-J, Quadakkers WJ. Effect of specimen thickness on chromia scaling of Ni25Cr in N2–O2–H2O test gases at 1000 °C. Mater High Temp 2015;32(1-2):160–6. https://doi.org/10.1179/0960340914Z.00000000092.
- [34] Hansel M, Shemet V, Markus T. Varying growth stress to study how H2O affect chromia scaling in high pO2 gas at 900 °C. Mater Lett 2018;233:51–4.
- [35] ASTM E647-11, Standard Test Method for Measurement of Fatigue Crack Growth Rates, ASTM International, West Conshohocken, PA; 2011, www.astm.org.
- [36] Schone D, Zerbst U, Madia M. Experimentelle Ermittlung des Schwellenwertes ΔKth mittels unterschiedlicher Methoden und für verschiedene Spannungsverhältnisse. Proc. DVM-AK Bruchvorgange, Freiberg/Sa., 2015.
- [37] Pokluda J, Pippan R. Analysis of roughness-induced crack closure based on asymmetric crack-wake plasticity and size ratio effect. Mater Sci Eng. A 2007;462:355–8.
- [38] Tracey DM. Journal of engineering materials and technology. ASME Trans 1976;98:146.